

Received:  
5 February 2014Revised:  
7 April 2014Accepted:  
14 April 2014

doi: 10.1259/bjr.20140123

Cite this article as:

Somarouthu BS, Shinagare AB, Rosenthal MH, Tirumani H, Hornick JL, Ramaiya NH, et al. Multimodality imaging features, metastatic pattern and clinical outcome in adult extraskeletal Ewing sarcoma: experience in 26 patients. *Br J Radiol* 2014;87:20140123.

## FULL PAPER

# Multimodality imaging features, metastatic pattern and clinical outcome in adult extraskeletal Ewing sarcoma: experience in 26 patients

<sup>1</sup>B S SOMAROUTHU, MB BS, <sup>1,2</sup>A B SHINAGARE, MD, <sup>1,2</sup>M H ROSENTHAL, MD, PhD, <sup>1</sup>H TIRUMANI, MB BS, <sup>3</sup>J L HORNICK, MD, PhD, <sup>1,2</sup>N H RAMAIYA, MD and <sup>1,2</sup>S H TIRUMANI, MD

<sup>1</sup>Department of Imaging, Dana-Farber Cancer Institute, Harvard Medical School, Boston, MA, USA

<sup>2</sup>Department of Radiology, Brigham and Women's Hospital, Harvard Medical School, Boston, MA, USA

<sup>3</sup>Department of Pathology, Brigham and Women's Hospital, Harvard Medical School, Boston, MA, USA

Address correspondence to: Dr Sreeharsha Tirumani

E-mail: [sreeharsha\\_tirumani@DFCI.harvard.edu](mailto:sreeharsha_tirumani@DFCI.harvard.edu)

**Objective:** To describe the multimodality imaging features, metastatic pattern and clinical outcome in adult extraskeletal Ewing sarcoma (EES).

**Methods:** In this institutional review board-approved, health insurance portability and accountability act-compliant retrospective study, we included 26 patients (17 females and 9 males; mean age, 36 years; range, 18–85 years) with pathologically confirmed EES seen at our institute between 1999 and 2011, who had imaging of primary tumour. Imaging of primary tumour in all 26 patients and follow-up imaging in 23 was reviewed by two radiologists in consensus. Clinical data were extracted from electronic medical records.

**Results:** The most common primary sites were the torso ( $n = 13$ ), extremities ( $n = 10$ ) and head and neck (HN) region ( $n = 3$ ). The mean tumour size was 9 cm (range, 3–22 cm); tumours of the torso were larger than those of other areas ( $p > 0.05$ ). Compared with the skeletal muscle, tumours were isodense on CT (21/21), hypointense ( $n = 5$ )

to isointense ( $n = 14$ ) on  $T_1$  weighted image, hyperintense on  $T_2$  weighted image (19/19) and were fluorine-18 fludeoxyglucose ( $^{18}\text{F}$ -FDG)-avid [10/10; mean maximum standardized uptake value of 7 (range, 3–11)]. Necrosis (15/26), haemorrhage (5/26) and adjacent organ invasion (14/26) were present without calcification. Median follow-up was 16 months. 5 patients had local recurrence (torso, 3; extremity, 1; and HN, 1). Metastases developed in 11 patients (torso, 7; extremities, 3; and HN, 1;  $p > 0.05$ ); 8 at presentation, most commonly to lung (9/11), peritoneum (4/11), muscles (4/11) and lymph nodes (4/11). Nine patients (torso, 7; extremity, 1; and HN, 1) died (10 months median survival) ( $p > 0.05$ ).

**Conclusion:** Adult EESs are large tumours, which frequently invade adjacent organs and metastasize to the lung. EESs of the torso are larger, have more frequent metastases and poorer outcomes.

**Advances in knowledge:** Adult EESs of the torso have poor outcomes compared with other EESs.

Ewing sarcoma (EES) is an aggressive, high-grade rounded cell sarcoma characterized by the t(11; 22) (q24; q12) chromosomal translocation, which fuses the *EWSR1* gene on chromosome 22p12 with the *FLI1* gene on chromosome 11q24 in 85–90% of cases.<sup>1</sup> The transcriptional product of this translocation upregulates insulin-like growth factor 1 (IGF1), a key factor in cell proliferation.<sup>2</sup> By immunohistochemistry, these tumours are characterized by strong membranous expression of CD99.<sup>3</sup> The terms peripheral primitive neuroectodermal tumour (PNET) and Askin tumour (thoracopulmonary PNET) are no longer used; these tumours are identical to EES.<sup>4</sup>

Data from the Surveillance, Epidemiology and End Results (SEER) report an overall incidence of one case of

EES per 1 million in the USA.<sup>5</sup> In the UK, EES is the second most common sarcoma accounting for 39% of childhood bone sarcomas with an estimated incidence of 1.58–2.21 per million person years.<sup>6</sup> Most of the ESSs in the first two decades of life (up to 80%) occur in the skeleton.<sup>7</sup> On the contrary, extra-osseous origin is more common in adults than that in children with >50% of primary adult EESs being extra-osseous in origin.<sup>8</sup> Skeletal and extraskeletal EESs show differences in clinical presentation and outcomes.<sup>9</sup> Adult EESs tend to have poor prognosis with high incidence of local recurrence and distant metastases.<sup>3</sup> There have been significant advances in the management strategies of ESS, including the use of neoadjuvant chemotherapy and post-operative local radiation.<sup>3</sup> The development of monoclonal antibodies

such as figitumumab against IGF1 receptors has opened the window for new molecular-targeted therapies in EES.<sup>10</sup> The literature pertaining to the multimodality imaging features of adult EES and its metastatic pattern is scant. Accordingly, the purpose of our study was to describe the multimodality imaging features and metastatic pattern of EES, providing a correlation with clinical outcome.

## METHODS AND MATERIALS

### Subjects

This is a Health Insurance Portability and Accountability Act (HIPAA)-compliant, institutional review board-approved retrospective study with a waiver for informed consent. We identified 26 adult patients (17 females and 9 males; mean age, 36 years; range, 18–85 years) with pathologically confirmed diagnosis of EES and imaging of the primary tumour available for review, who were seen at our institution between January 1999 and December 2011.

### Imaging

Pre-treatment imaging of primary tumours in all the 26 patients included MRI in 19 patients, 15 with intravenous gadolinium; CT scans in 21 patients, 16 with intravenous contrast; and fluorine-18 fludeoxyglucose (<sup>18</sup>F-FDG) positron emission tomography (PET)/CT in 10 patients. Follow-up imaging was available in 23 patients and included CT in 21 patients, MRI in 16 patients and <sup>18</sup>F-FDG PET/CT in 7 patients. In total, we reviewed 198 CT, 143 MRI and 26 PET/CT examinations.

### Image analysis

All the images were reviewed in consensus by two oncoradiology fellowship-trained radiologists with 7 and 15 years' experience each. The following features were noted for each tumour: location, size, margins, the presence of necrosis, haemorrhage, calcification, mass effect, bone destruction, local invasion and distant metastases. On the CT images, tumour attenuation, homo-/heterogeneity and enhancement with respect to the paraspinal muscles were noted. MRI features including signal intensity on  $T_1$  and  $T_2$  weighted images as compared with the paraspinal muscles, homo-/heterogeneity, post-gadolinium enhancement (less than, similar to or greater than skeletal muscles) were recorded. On PET/CT images, the metabolic activity of the tumours in terms of the maximum standardized uptake value (SUVmax) was noted. On follow-up imaging, the development of locoregional recurrence and sites of distant metastases were recorded.

### Management and outcome

The clinical information for all the 26 patients, including the date of diagnosis, demographic data, type of management (chemotherapy, surgery and radiotherapy) and outcome, including death, was documented from the electronic medical records. The average duration of follow-up, the date of last follow-up, date of detection of distant metastases and the date of death were also recorded. The histopathological features of resected specimens, especially the presence or absence of positive margins, were noted for all the surgically resected tumours.

### Statistical analysis

The results were statistically analysed to correlate tumour location and size with metastases and outcome using the Mann-Whitney  $U$  test and Fisher's exact using GraphPad Prism v. 6; (GraphPad Prism Software Inc., La Jolla, CA). A  $p$ -value  $<0.05$  was considered statistically significant.

## RESULTS

The mean age of our study population was 36 years with a range of 18–85 years. Of the 26 patients, 13 (50%) had EES in the torso [chest ( $n = 4$ ), abdomen ( $n = 7$ ) and pelvis ( $n = 2$ )], 10 (38%) in the extremities and 3 (12%) in the head and neck (HN;  $n = 3$ ).

EESs in the chest were seen as paraspinal mass ( $n = 1$ ), pleural-based tumour ( $n = 1$ ), chest wall mass ( $n = 1$ ) and as a mediastinal mass ( $n = 1$ ). Tumours in the abdomen were located in the retroperitoneum ( $n = 6$ ) and small bowel mesentery ( $n = 1$ ), with four of the retroperitoneal tumours involving the adrenal gland and/or kidney (Figure 1). Of the ten EESs in the extremities, three were seen in the upper extremity, three in the thigh, three in the gluteal muscles and one along the sciatic nerve (Figure 2). Of the three EESs in the HN, one was seen in the brain, one in the right supraclavicular region and one in the pre-vertebral location in the lower neck.

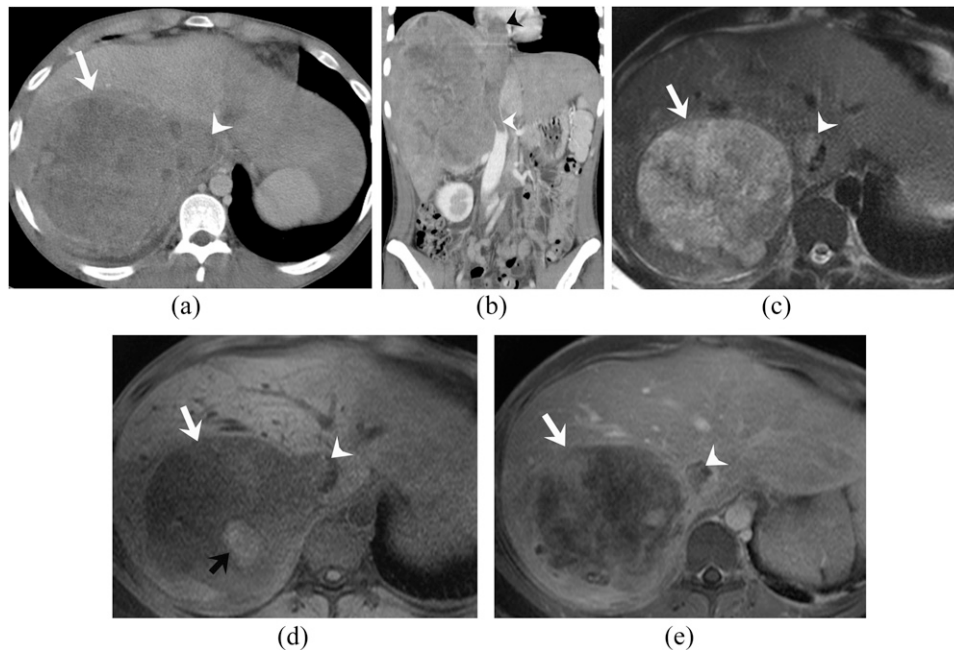
### Imaging features of primary extraskelatal Ewing sarcomas

The mean largest dimension of EES was 9 cm (range, 3–22 cm). The tumours involving the torso were larger in size with a mean size of 14 cm than those of the tumours in the extremities, which had a mean size of 8 cm ( $p > 0.05$ ). Of the 13 tumours in the torso, 5 had ill-defined infiltrative margins. All the tumours involving the extremities and the HN had well-defined margins except one tumour involving the buttock, which had infiltrative margins. On CT scan ( $n = 21$ ), 17 tumours were isodense to the skeletal muscles with heterogeneous attenuation, while 4 tumours were homogeneous. After intravenous contrast administration ( $n = 16$ ), all the tumours showed heterogeneous enhancement (Figure 1). None of the tumours showed calcification on the CT scan.

On MRI ( $n = 19$ ), compared with skeletal muscles, 5 tumours were hypointense and 14 tumours were isointense on  $T_1$  weighted images. All the tumours were heterogeneously hyperintense on  $T_2$  weighted images except one tumour in the arm, which was homogeneously  $T_2$  hyperintense. Post-gadolinium images ( $n = 15$ ) showed enhancement less than or similar to the skeletal muscles in 11 tumours and more than the skeletal muscle in 4 tumours (Figures 1 and 2). Haemorrhage was seen on MRI as areas of  $T_1$  hyperintensity in 5 tumours (19%). There was CT/MR evidence of necrosis in 15/26 (58%) tumours. On <sup>18</sup>F-FDG PET/CT ( $n = 10$ ), all the tumours were <sup>18</sup>F-FDG-avid with mean SUVmax of 7 (range, 3–12) (Figure 2).

There was mass effect on adjacent organs in all the tumours; however, the invasion of the adjacent viscera or neurovascular structures was noted in 14 tumours (54%). In the abdomen, the invasion of the kidney was noted in four patients and of the liver and spleen in one patient each. Bone destruction was noted in

Figure 1. A 24-year-old man with primary retroperitoneal (adrenal) extraskeletal Ewing sarcoma. (a, b) Axial and coronal reformatted contrast-enhanced CT images of the abdomen reveal a large heterogeneous enhancing right adrenal mass (white arrow) with contiguous tumour thrombus in the inferior vena cava (IVC) (white arrowheads) extending up to the right atrium (black arrowhead). The adjacent liver parenchyma is invaded at places. (c–e) Axial  $T_2$  weighted, pre- and post-gadolinium fat-suppressed  $T_1$  weighted MRI images demonstrate the mass to be heterogeneously hyperintense on  $T_2$  weighted images and hypointense on  $T_1$  weighted images (white arrows) with heterogeneous enhancement, haemorrhage in the form of  $T_1$  hyperintense areas (black arrow) and enhancing tumour thrombus in the IVC (white arrowheads).



one tumour involving the chest wall. Complications that were noted on imaging included neural foraminal extension ( $n = 2$ ), spinal cord compression ( $n = 1$ ), tumour enteric fistula ( $n = 1$ ), and invasion of inferior vena cava (IVC) ( $n = 2$ ), renal vein ( $n = 1$ ) and adrenal vein ( $n = 1$ ). Intra-abdominal extension of an extremity EES was noted in one patient.

#### Imaging of recurrent and metastatic extraskeletal Ewing sarcomas

Of the 23 patients who had follow-up imaging, 5 patients (22%) developed local recurrence of the disease at the time of the last follow-up, with 5 of them showed distant metastases as well. Surgical margins were positive in four of these patients at the time of resection. Sites of local recurrence were the torso, 3 (25%) (retroperitoneum, mediastinum, pelvis); extremities, 1 (12.5%); and HN, 1 (33%) ( $p > 0.05$ ). The recurrent tumours were similar to the primary tumours on imaging.

Distant metastases were seen in 11/23 patients (48%) with follow-up imaging; 8 of them (35%) had metastases at presentation. The distribution of metastases according to the site were torso, 7/12 (58%); extremities, 3/8 (38%); and HN, 1/3 (33%) ( $p > 0.05$ ). The most common sites of metastases were to the lung (nine patients, 27%), peritoneal cavity (four patients, 12%), muscles (four patients, 12%) and lymph nodes (four patients, 12%) (Table 1).

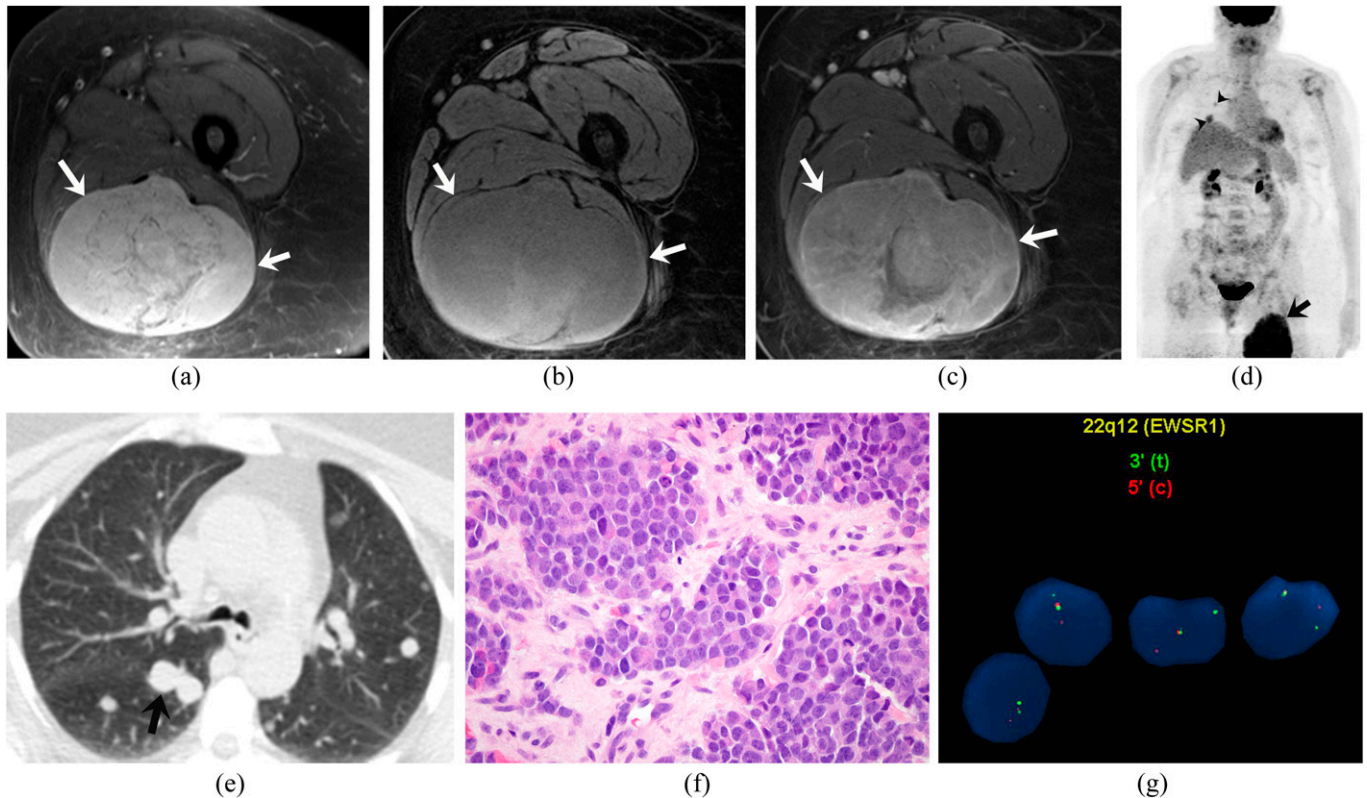
Lung metastases were seen in three patients each with primary tumours in the abdomen and extremities, two in the chest and

one in the supraclavicular region. The lung metastases were seen as numerous bilateral pulmonary nodules ranging in size from 0.5 to 10 cm (mean, 3.1 cm; median, 1.5 cm) in seven patients and as a single lesion of 0.6 and 5.0 cm in the remaining two patients (Figure 2). Peritoneal metastases were seen as large peritoneal nodules and masses in three patients and perihepatic implants in one patient. Ascites were seen in one patient with peritoneal metastases. Metastatic lymph nodes ranged in size from 1.0 to 3.0 cm, with necrosis in the larger nodes. PET/CT imaging in seven patients demonstrated distant metastases in four patients. All the metastatic lesions were  $^{18}\text{F}$ -FDG-avid with mean SUVmax of 5 (range, 3–14) (Figure 2). All the  $^{18}\text{F}$ -FDG-avid metastases had CT correlates except for bone metastases in one patient, which remained occult on the CT.

#### Management and outcome

Of the 26 patients, 17 underwent surgical resection of the tumour after neoadjuvant chemotherapy, 4 patients were treated with primary radiotherapy with concurrent chemotherapy and 5 patients were treated with only chemotherapy. All of the 17 patients who were treated with surgery received adjuvant chemotherapy, while 14/17 patients received additional adjuvant radiotherapy. Surgical margins were positive in 4/17 patients, all of whom developed local tumour recurrence. Clinical follow-up was available in 23 patients, while 3 patients were lost to follow-up. The median duration of follow-up was 16 months (range, 6–166 months). At the time of last follow-up, 9/23 patients on follow-up died at a median interval of 10 months (range, 6–20 months) from

Figure 2. A 63-year-old woman with extraskeletal Ewing sarcoma of the thigh. (a–c) Axial fat-suppressed  $T_2$  weighted, pre- and post-gadolinium fat-suppressed  $T_1$  weighted MRI images demonstrate a heterogeneously hyperintense mass on  $T_2$  weighted images (arrows), which is heterogeneously isointense on  $T_1$  weighted images with heterogeneous enhancement. (d) Coronal maximum intensity projection image of fluorine-18 fludeoxyglucose ( $^{18}\text{F}$ -FDG) positron emission tomography/CT FDG uptake (maximum standardized uptake value of 12) in the right thigh mass (arrow) and multiple  $^{18}\text{F}$ -FDG-avid pulmonary metastases (arrowheads). (e) Axial CT image of the chest confirms the pulmonary metastases (arrow). (f). Haematoxylin and eosin staining (original magnification  $\times 600$ ) of the biopsy specimen of the tumour demonstrates sheets of uniform rounded cells with scant cytoplasm. (g). Fluorescence *in situ* hybridization analysis using break-apart probes directed against the 5' and 3' ends of the *EWSR1* gene shows *EWSR1* gene rearrangement.



the date of diagnosis. Of these nine patients, seven had EES in the torso (7/12 patients with follow-up, 58%), while one each had EES in the extremities (1/8 patients with follow-up, 13%) and HN (1/3 patients with follow-up, 33%) ( $p > 0.05$ ).

## DISCUSSION

The mean age of presentation of adult EES in our study was 36 years. This is in contrast to earlier reports of a younger age of presentation at 18–24 years.<sup>3,11–13</sup> There was also slight female preponderance in our series, compared with slight male preponderance in earlier studies.<sup>9,13</sup> In an analysis of the SEER database between 1973 and 2007, Applebaum *et al*<sup>9</sup> found that patients with EES ( $n = 683$ ) were older and less likely to be male than patients with skeletal ESS ( $n = 1519$ ). They found a bimodal distribution of EES with most tumours occurring in patients older than 35 years or younger than 5 years.

EES can occur virtually anywhere in the body and can be classified into central/trunk and peripheral/extremity EESs, with most of the earlier studies reporting higher prevalence of central EESs.<sup>3,11–13</sup> There was near equal distribution of EES between the torso ( $n = 13$ ) and the extremities ( $n = 10$ ) in our study. In

the extremities, most EESs in our study occurred in the gluteal region and thighs. In the torso, a greater number of patients had abdominal EES, especially in the retroperitoneum involving the kidneys and adrenal glands. By contrast, most of the earlier studies report the chest wall to be the most common site for EES in the torso.<sup>13–15</sup> The higher incidence of abdominal EES in our study might be related to referral bias. An HN presentation of EES is rare (3/26 cases in our study).

The median tumour size in our study was 9 cm with the tumours in the torso (mean size, 14 cm) larger than extremity tumours (mean size, 8 cm) ( $p > 0.05$ ). Although not statistically significant, this is in agreement with earlier reports<sup>3,8</sup> and is explained by the fact that tumours of the torso often have insidious onset and delayed presentation. The size is an important predictor of survival, with large size at presentation being an adverse prognostic factor. El Weshi *et al*<sup>3</sup> in their study of 57 adult patients with EES found that tumours  $< 10$  cm had favourable survival.

Imaging features of EES are non-specific. Compared with skeletal muscle, most of the tumours in our study were isodense on CT, hypointense on  $T_1$  weighted images and heterogeneously



Table 1. Distribution of metastatic lesions in extraskeletal Ewing sarcoma ( $n = 11$ )

Site	Number	Percentage
Lung	9	26.5
Peritoneum	4	11.8
Muscles	4	11.8
Lymph nodes	4	11.8
Bone	3	8.8
Mesentery	3	8.8
Subcutaneous	2	5.9
Liver	1	2.9
Bowel	1	2.9
Pancreas	1	2.9
Spleen	1	2.9
Brain	1	2.9
Total	34	

hyperintense on  $T_2$  weighted images with variable post-contrast enhancement (Figures 1 and 2). Similar to earlier observations, extensive necrosis and haemorrhage was noted especially in large tumours.<sup>16</sup> Calcification is uncommon in EES occurring in <10% cases.<sup>8,15</sup> None of the tumours in our series demonstrated calcification. We observed that tumours in the abdomen had a greater tendency to have infiltrative margins with invasion of the adjacent structures than those of peripheral EESs. EESs tend to displace adjacent structures rather than encase them; this can be best assessed by CT or MRI. Although mass effect on the adjacent structures was present in all the tumours in our series, the invasion of adjacent structures was noted in about 14/26 cases. PET/CT has very high sensitivity and specificity of 96% and 92%, respectively, for detecting EESs.<sup>17</sup> Similar to skeletal ESSs, EESs are  $^{18}\text{F}$ -FDG-avid tumours (Figure 2). The mean SUVmax of the primary tumours in our study was 7 (range, 3–11).

The differential diagnosis for thoracic EES in adults includes lung cancer, lymphoma, other soft-tissue sarcomas, neurogenic tumours and metastases. EESs of the retroperitoneum are difficult to differentiate from other retroperitoneal tumours in adults. Invasion of the renal vein, IVC and the liver are seen in both EES and renal cell carcinoma (RCC) or adrenocortical carcinoma (ACC). Features that can help in differentiating retroperitoneal EES from RCC or ACC are an earlier age of presentation, the absence of metastatic lymphadenopathy and the absence of calcification in EES, which can be seen in 10–30% cases of RCC and ACC.<sup>16</sup> Abdominal EESs are most likely unilateral, and do not cross the midline. EESs of the extremities in our study were indistinguishable from other extremity soft-tissue sarcomas and were seen as well circumscribed tumours with variable degrees of necrosis. The relatively small size of peripheral EESs in our study can be explained by their earlier clinical presentation. HN involvement by EES is uncommon,

accounting for approximately 12% cases of EESs and occurs as orbital, extradural or cervical masses.<sup>8</sup>

EESs are aggressive tumours with high propensity for local recurrence and distant metastases. The incidence of local recurrence in our study (5/23, 22%) was less than the incidence reported by El Weishi et al<sup>3</sup> in 57 adult patients with EES (36%). The incidence of metastases at 48% (11/23) in our study was higher than those in earlier reports of adult EESs, which may be related to referral bias. There were a greater number of metastases in patients with EES of torso (58% vs 38% in extremities and 33% in HN EES), although this was not statistically significant.

A significant number of patients in our study (8/23, 35%) also had metastatic disease at presentation, similar to the study by Tao et al<sup>18</sup> of 37 patients who found metastases at presentation in 43% patients, indicating the necessity for complete staging at the time of initial diagnosis. The most common site of metastases in our study was the lung (27%), which is in agreement with the existing literature.<sup>3,14,15</sup> The other common sites of metastases in our study were the peritoneal cavity, muscles and lymph nodes. The lymph node involvement was noted in 4/11 patients with metastases, similar to the study by El Weishi et al<sup>3</sup> (5/18). PET/CT has been shown to be useful for detecting distant metastases, especially bone metastases, which can remain occult on CT. The sensitivity and specificity of PET/CT for staging and restaging in the study of 53 patients with EES by Gerth et al<sup>19</sup> was 87% and 97%, respectively, with an accuracy of 94%.<sup>19</sup>

Owing to its rarity, the optimal management of EES is uncertain. Aggressive management with multimodality treatment is recommended to improve survival rates.<sup>18,20</sup> The high incidence of local recurrence in earlier series was owing to the lack of post-operative radiotherapy.<sup>3</sup> The 5-year survival in the study by El Weishi et al<sup>3</sup> was 46% with 35 deaths out of 57 patients. The 3-year survival in the study by Tao et al<sup>18</sup> was 43%. Of the 23 patients under follow-up in our study, 9 (39%) were deceased at the time of the last follow-up at a median interval of 10 months (range, 6–20 months). Although the relation between the site of primary tumour and outcome is controversial (some studies concluding adverse prognosis for central tumours, while others do not<sup>14,21</sup>), we observed that EESs in the torso had a greater number of local recurrences, metastases and deaths than that of peripheral EESs, although this was not statistically significant.<sup>14</sup> The explanation for this observation is unknown but has been presumed to be related to the large size of tumours of the torso at presentation.<sup>14</sup>

The limitations of our study include relatively small sample size and referral bias of our study population. A significant number of patients in our database were excluded from the study owing to non-availability of imaging of the primary tumour. Patients who are referred to our large sarcoma treatment group are often initially worked up at outside hospitals before referral. This referral bias also explains a relatively higher incidence of metastases in our cohort. We were unable to support the observations in our study statistically owing to the small number of patients in individual groups of EES.

## CONCLUSION

In conclusion, we present the multimodality imaging features of adult EES in 26 patients. Typical imaging characteristics of EES include large heterogeneous tumours of the torso or the extremities, which can show necrosis, haemorrhage and

adjacent organ invasion and lack calcification. EESs can metastasize to the lungs, peritoneum, muscles and lymph nodes. Compared with extremity and HN EESs, EESs of the torso are larger, have more frequent metastases and have poorer outcomes.

## REFERENCES

1. Quesada J, Amato R. The molecular biology of soft-tissue sarcomas and current trends in therapy. *Sarcoma* 2012; **2012**: 849456. Available from: <http://www.ncbi.nlm.nih.gov/pubmed/22665999>. doi: 10.1155/2012/849456
2. Juergens H, Daw NC, Geoerger B, Ferrari S, Villarroel M, Aerts I, et al. Preliminary efficacy of the anti-insulin-like growth factor type 1 receptor antibody figitumumab in patients with refractory Ewing sarcoma. *J Clin Oncol* 2011; **29**: 4534–40. doi: 10.1200/JCO.2010.33.0670
3. El Weshi A, Allam A, Ajarim D, Al Dayel F, Pant R, Bazarbashi S, et al. Extraskelatal Ewing's sarcoma family of tumours in adults: analysis of 57 patients from a single institution. *Clin Oncol (R Coll Radiol)* 2010; **22**: 374–81. doi: 10.1016/j.clon.2010.02.010
4. Murphey MD, Senchak LT, Mambalam PK, Logie CI, Klassen-Fischer MK, Kransdorf MJ. From the radiologic pathology archives: ewing sarcoma family of tumors: radiologic-pathologic correlation. *Radiographics* 2013; **33**: 803–31.
5. Jawad MU, Cheung MC, Min ES, Schneiderbauer MM, Koniaris LG, Scully SP. Ewing sarcoma demonstrates racial disparities in incidence-related and sex-related differences in outcome: an analysis of 1631 cases from the SEER database, 1973–2005. *Cancer* 2009; **115**: 3526–36. doi: 10.1002/cncr.24388
6. Eyre R, Feltbower RG, Mubwandarikwa E, Jenkinson HC, Parkes S, Birch JM, et al. Incidence and survival of childhood bone cancer in northern England and the West Midlands, 1981–2002. *Br J Cancer* 2009; **100**: 188–93. doi: 10.1038/sj.bjc.6604837
7. Maki RG. Pediatric sarcomas occurring in adults. *J Surg Oncol* 2008; **97**: 360–8. doi: 10.1002/jso.20969
8. Javery O, Krajewski K, O'Regan K, Kis B, Giardino A, Jagannathan J, et al. A to Z of extraskelatal Ewing sarcoma family of tumors in adults: imaging features of primary disease, metastatic patterns, and treatment responses. *AJR Am J Roentgenol* 2011; **197**: W1015–22. doi: 10.2214/AJR.11.6667
9. Applebaum MA, Worch J, Matthey KK, Goldsby R, Neuhaus J, West DC, et al. Clinical features and outcomes in patients with extraskelatal Ewing sarcoma. *Cancer* 2011; **117**: 3027–32. doi: 10.1002/cncr.25840
10. Tirumani SH, Jagannathan JP, O'Regan K, Kim KW, Shinagare AB, Krajewski KM, et al. Molecular targeted therapies in non-GIST soft tissue sarcomas: what the radiologist needs to know. *Cancer Imaging* 2013; **13**: 197–211. doi: 10.1102/1470-7330.2013.0022
11. Ahmad R, Mayol BR, Davis M, Rougraff BT. Extraskelatal Ewing's sarcoma. *Cancer* 1999; **85**: 725–31.
12. Rud NP, Reiman HM, Pritchard DJ, Frassica FJ, Smithson WA. Extrasosseous Ewing's sarcoma. A study of 42 cases. *Cancer* 1989; **64**: 1548–53.
13. Tural D, Molinas Mandel N, Dervisoglu S, Oner Dinbas F, Koca S, Colpan Oksuz D, et al. Extraskelatal Ewing's sarcoma family of tumors in adults: prognostic factors and clinical outcome. *Jpn J Clin Oncol* 2012; **42**: 420–6. doi: 10.1093/jcco/hys027
14. Baldini EH, Demetri GD, Fletcher CD, Foran J, Marcus KC, Singer S. Adults with Ewing's sarcoma/primitive neuroectodermal tumor: adverse effect of older age and primary extrasosseous disease on outcome. *Ann Surg* 1999; **230**: 79–86.
15. Dick EA, McHugh K, Kimber C, Michalski A. Imaging of non-central nervous system primitive neuroectodermal tumours: diagnostic features and correlation with outcome. *Clin Radiol* 2001; **56**: 206–15. doi: 10.1053/crad.2000.0614
16. Hari S, Jain TP, Thulkar S, Bakhshi S. Imaging features of peripheral primitive neuroectodermal tumours. *Br J Radiol* 2008; **81**: 975–83. doi: 10.1259/bjr/30073320
17. Treglia G, Salsano M, Stefanelli A, Mattoli MV, Giordano A, Bonomo L. Diagnostic accuracy of <sup>18</sup>F-FDG-PET and PET/CT in patients with Ewing sarcoma family tumours: A systematic review and a meta-analysis. *Skeletal Radiol* 2012; **41**: 249–56.
18. Tao HT, Hu Y, Wang JL, Cheng Y, Zhang X, Wang H, et al. Extraskelatal Ewing sarcomas in late adolescence and adults: a study of 37 patients. *Asian Pac J Cancer Prev* 2013; **14**: 2967–71.
19. Gerth HU, Juergens KU, Dirksen U, Gerss J, Schober O, Franzius C. Significant benefit of multimodal imaging: PET/CT compared with PET alone in staging and follow-up of patients with Ewing tumors. *J Nucl Med* 2007; **48**: 1932–9. doi: 10.2967/jnumed.107.045286
20. Venkitaraman R, George MK, Ramanan SG, Sagar TG. A single institution experience of combined modality management of extra skeletal Ewings sarcoma. *World J Surg Oncol* 2007; **5**: 3. doi: 10.1186/1477-7819-5-3
21. Sailer SL, Harmon DC, Mankin HJ, Truman JT, Suit HD. Ewing's sarcoma: surgical resection as a prognostic factor. *Int J Radiat Oncol Biol Phys* 1988; **15**: 43–52